Paper

GAS MIXING FOR ACHIEVING SUITABLE CONDITIONS FOR SINGLE POINT AEROSOL SAMPLING IN A STRAIGHT TUBE: EXPERIMENTAL AND NUMERICAL RESULTS

M. Anand, A. R. McFarland, and K. R. Rajagopal*

Abstract—**Experimental measurements of velocity and tracer gas concentration are taken in a straight tube to evaluate the effectiveness of mixing in achieving conditions as required by ANSI N13.1-1999 for single point extractive sampling from stacks and ducts of nuclear facilities. Mixing is evaluated for inlet turbulent intensities of 1.5%, 10%, and 20%, achieved by introducing various bi-plane grids, and for conditions generated by a commercial static gas mixer. The data obtained (at Reynolds number = 15,000) highlight the importance of inlet turbulence intensity in the process of turbulent dispersion of a dilute gas. The gas mixer does not introduce significant pressure losses and unlike bi-plane grids, the turbulence downstream of the mixer is not homogenous. A judicious choice of the release location that uses the large scale eddies and inhomogeneity of the turbulence ensures that the specified ANSI N13.1-1999 criteria are attained within 7 diameters downstream of the duct inlet. This is significantly more effective than a bi-plane grid where even with 20% inlet intensity the criteria are met only at 21 diameters downstream. The predictions of a proposed semi-empirical correlation match favorably with data. For example, at 18 diameters downstream with inlet intensities of 1.5% and 10%, the predicted coefficients of variation (COVs) of 150% and 65% are close to the actual values of 154% and 50%; where the COV of a set of measurements is the ratio of the standard deviation of the set to its mean value. The corresponding results obtained using commercially available software are 141% and 12%. Results from a particle-tracking model show good qualitative trends, but they should not be used to determine compliance with the requirements of the ANSI standard.**

Health Phys. 84(1):82–91; 2003

Key words: emissions, atmospheric; air sampling; monitoring, air; sampling

INTRODUCTION

REGULATIONS THAT govern radionuclide air emissions from stacks and ducts of Federal nuclear facilities are specified by the U.S Environmental Protection Agency (EPA), and these mandate continuous emission sampling (CES) for stacks and ducts that can potentially emit significant quantities of radionuclides into the atmosphere (U.S. EPA 2001c, d). The U.S. EPA presently requires that sampling of radionuclides from stacks and ducts follow the protocol of the American National Standards Institute (ANSI) Standard N13.1-1969 (ANSI 1969) at a location complying with the requirements of 40CFR60, Appendix A (U.S. EPA 2001a, b). The ANSI standard has undergone a significant revision (Health Physics Society 1999), which aims to replace the prescriptive nature of some guidelines by more suitable performance-based ones. Included in the recommendations of the current standard is the use of single point extractive sampling from a location in a stack or duct where both the fluid momentum and contaminant concentration are relatively uniform across the cross section of the stack or duct. Currently, the U.S. EPA is considering how to replace ANSI N13.1-1969 with ANSI N13.1-1999, and, while this review is taking place, U.S. DOE facilities are permitted to use Alternate Reference Methodologies (U.S. EPA 1994) that embody the principles for aerosol sampling found in the new ANSI N13.1.

CES systems in nuclear applications typically provide aerosol samples that are integrated over approximately 1-wk periods. Deficiencies in methodology for continuous sampling with ANSI N13.1-1969 prompted the revision of the ANSI standard. In this context, McFarland and Rodgers (1993) proposed the Alternate Reference Methodologies. These recommendations, along with the changes in the ANSI standard, provide for better guidance in the design and operation of sampling systems.

Single point sampling, as recommended in the Alternate Reference Methodologies (ARM) and the revised ANSI standard, has substantial advantages compared with rakes of multiple isokinetic nozzles, which were previously acceptable technology. However, to comply with the requirements of the new ANSI standard,

* Department of Mechanical Engineering Texas A&M University College Station, TX.

For correspondence or reprints contact: A. R. McFarland at the above address, or email at arm@tamu.edu.

(*Manuscript received* 28 *November* 2001; *revised manuscript received* 1 *April* 2002, *accepted* 6 *August* 2002)

0017-9078/03/0

and for single point sampling to be applicable, the velocity and contaminant concentration profiles must be nearly uniform at the sampling location. While in some cases the stack or duct design will be such that the mixing is complete at a candidate sampling location, in others it may be necessary to engineer the flow to achieve this objective. It is thus important to have an idea of the degree of mixing that can be obtained in typical stack or duct configurations.

In this study, experimental data are obtained for mixing in straight pipes and are used to develop a correlation to characterize the degree of mixing in a straight pipe. The results presented herein serve to illustrate the importance of inlet turbulence and turbulent kinetic energy (as quantified by the turbulent intensity) over Reynolds number in the turbulent dispersion of dilute gases. A tracer (SF_6, 0.1% v/v in air) is released by means of a small circular tube (0.6 mm internal diameter) located coaxially at various release locations in the mainstream flow similar to a jet. The ratio of tracer gas jet speed to wind tunnel air speed is maintained at 0.2, a value for which the jet is underexpanded and thereby does not show initial expansion-induced dispersion. The experimental data are compared with numerical simulations performed with FLUENT software (FLUENT Version 5.4, Lebanon, NH) to evaluate the possibility of using commercially available particle-tracking models to predict mixing.

A few studies have been carried out on mixing in straight ducts following static mixing elements (Baker 1991; Cybulski and Werner 1986; Pahl and Muschelknautz 1982). These studies do not deal with velocity and contaminant concentration profiles over the center 2/3 (~67%) of the cross sectional area of ducts (as required by the ANSI standard), and hence their results cannot be used to determine compliance with stack mixing criteria. A recent review of the sampling methodology for compliance with the ANSI standard was undertaken by Los Alamos National Laboratory (McFarland 1998), and field tests of mixing have been conducted on a stack at Los Alamos by Rodgers et al. (1996). Hampl et al. (1986) tested the mixing in straight ducts with some of the test configurations involving mixing elements upstream of ducts. Tracer gas was discharged from one to four points in the upstream region of the configurations. However, there were no bell mouths at the entrance of the duct mixing element configurations and this led to flow separation at the entrance, which caused artificial enhancement of mixing. The experimental results of Gupta (1999) make a clear case for such a line of thought. Significant differences are seen between the gas mixing results obtained with and without the flow straighteners. This suggests that the results of Hampl et al. (1986) cannot be used to infer compliance with the mixing requirements of the ANSI standard. It is seen that flow straighteners inhibit mixing of contaminants leading to longer duct length (and greater energy requirements) to ensure compliance with the mixing requirements of the ANSI standard. Langari (1997) presents some data for a straight pipe as a mixing element that are obtained at locations that conform to EPA Method 1. However, in his study, the tracer gas is introduced at a distance of approximately 10 diameters downstream of a flow straightener. Importantly, the exact flow conditions, vis-a-vis the nature of turbulence and the uniformity of velocity profile at the release location, are not easily captured because of the emphasis on a prescriptive guideline for the release location. In this regard, the data presented here document the flow development downstream of the release location and the mixing element (velocity profile, turbulent intensity and nature of turbulence) and correlate it with the gas mixing. The use of commercially available computational fluid dynamics software also allows us evaluate the suitability of the particle-tracking model for flow and gas mixing calculations. A similar procedure has been adopted by McFarland et al. (1997) who used a particle-tracking approach proposed by Abuzeid et al. (1991) to study the problem of aerosol deposition in bends and document the importance of turbulent fluctuations in the process. McFarland et al. (1999b) present experimental data for development of COVs in straight ducts downstream of some static mixing elements and bend configurations, and highlight the need for suitable predictive models for gas mixing. The numerical study and the semi-empirical correlation are steps in this direction.

EXPERIMENTAL SETUP AND METHODS

The experiments were conducted in a Schedule 40, PVC straight duct of inner diameter 152 mm (6 inch) fitted with a vacuum blower (Fig. 1). A bell mouth at the entrance of the pipe ensured a smooth flow transition and prevented flow separation in the duct entrance region. To create the condition of homogenous turbulence and uniform velocity at the inlet, various elements were introduced at the entrance of the pipe section. A steel screen, 8 × 8 mesh/inch, with a wire diameter of 1.19 mm (0.047 inch) and 38.9% open area (resistance coefficient ≅ 2.8, Laws and Livesey 1978) was fitted at the entrance of the bell mouth. This created a uniform time-mean velocity profile at the inlet of the bell mouth section. An additional steel screen (40 × 40 mesh/in) with a wire diameter of 0.254 mm (0.010 inch) and 36.0% open area (resistance coefficient ≅ 2.8) was

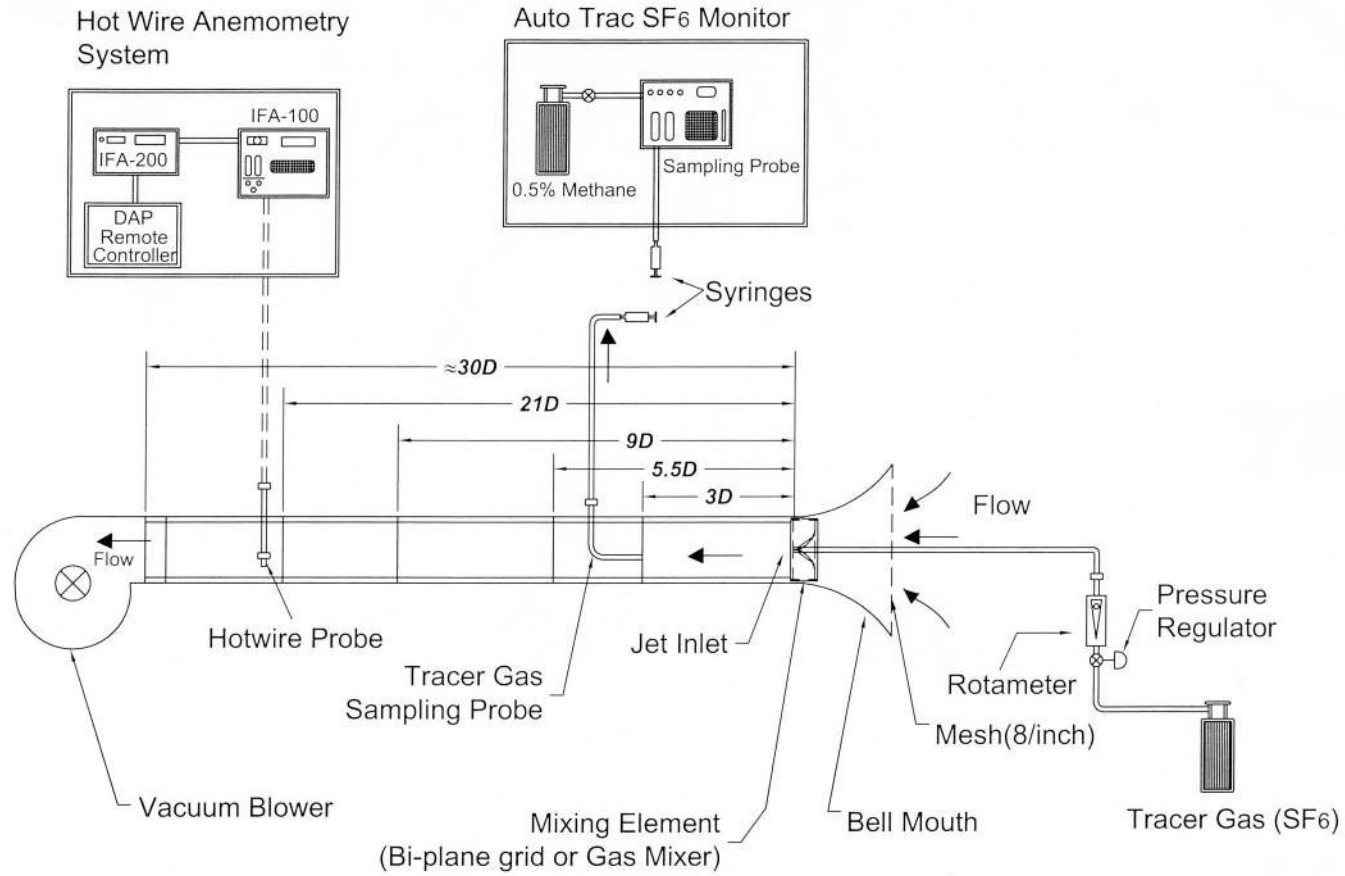

Fig. 1. Layout of the apparatus used to test various mixing elements with a straight pipe.

located at the beginning of the duct section. The turbulence just downstream of the latter screen had an intensity of 1.5%. Bi-plane grids (two arrays of parallel, uniformly spaced cylinders) were designed with a spacing-diameter ratio of 5.33 to generate turbulence intensities (at the inlet) of 10% and 20%. Grids with spacing of 25.4 mm (1 inch) and 50.8 mm (2 inch) were used to generate intensities of 10% and 20%, respectively. The gas mixer used in the test program was placed at the pipe entrance in lieu of the bi-plane grids, Fig. 2.

The experiments relate to some configurations that are encountered in the nuclear industry. Often, elements like flow straighteners or security grates are placed in a stack, which tend to reduce swirl, retard mixing, and create relatively uniform velocity conditions in straight duct configurations.

Experimental parameters

The principal variables considered are the COVs for velocity and tracer gas concentration and the mean turbulence intensity variation along the duct length (see Appendix for a list of symbols). At a mean velocity of 1.45 m s^{-1}, the pressure drop across the various bi-plane grids is about 5 to 10 Pa while that across the gas mixer is about 10 Pa (0.04 inches of water).

The coefficient of variation (COV) for any general variable ϕ is defined as

$$COV_\phi = \frac{\sqrt{\sum_{i=1}^{n}(\phi_i - \bar{\phi})^2}}{\bar{\phi}}, \qquad (1)$$

where

$$\bar{\phi} = \frac{\sum_{i=1}^{n} \phi_i}{n}. \qquad (2)$$

Here n is the number of sampling points. The COV is used for defining mixing criteria in the ANSI standard.

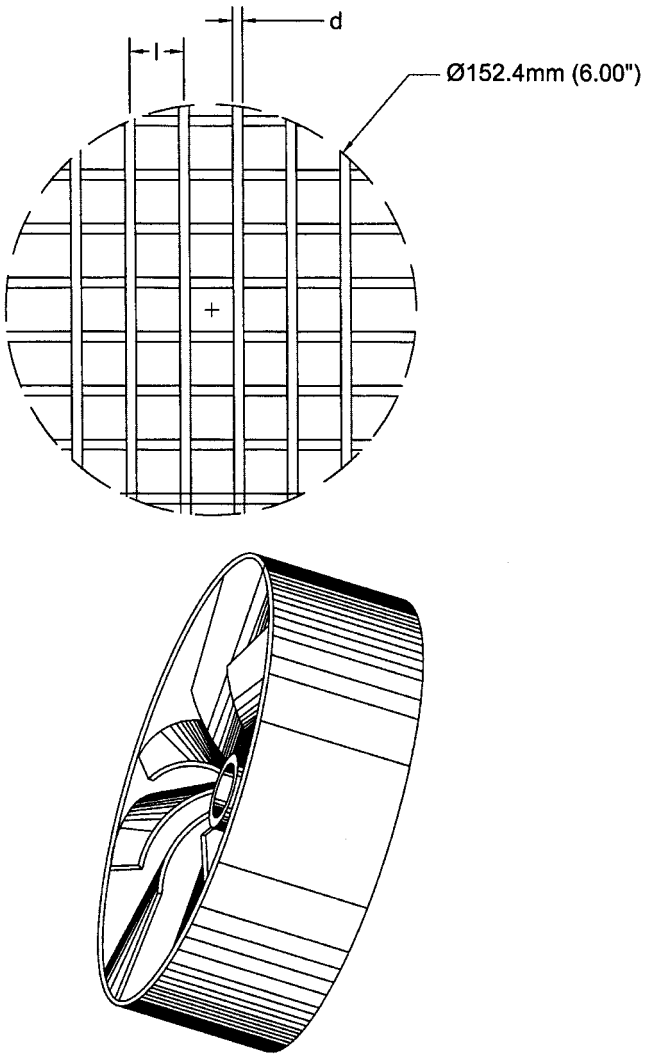

Fig. 2. Scale drawing of bi-plane grids (l/d = 5.33), and three-dimensional scale drawing of the commercial gas mixer.

Turbulence intensity (I), used to characterize turbulence in this study, is defined as

$$I = \frac{\sqrt{\overline{(u_z')^2}}}{\overline{U}_z}, \tag{3}$$

where u_z' represents the fluctuating component of the instantaneous velocity and $\bar{U}_z$ represents the time-averaged component of the instantaneous velocity, U_z (eqn 4):

$$U_z = \overline{U}_z + u_z'. \tag{4}$$

For a near one-dimensional flow situation, as in our case, the intensity (I) is directly proportional to the turbulent kinetic energy (k).

Sampling grid

The sampling grid (points across the duct cross section) used in this study is the 16 point EPA Method 1 velocity traverse grid (U.S EPA 2001a). The 16 traverse points are located at the centroids of equal area sectors of the duct cross sectional area. There is no traverse point at the center of the grid. However, in this study readings are taken at the center point to verify the symmetry of the velocity profile. The criterion on COVs, as specified by the ANSI, covers an area of the duct that encompasses not less than 2/3 (~67%) of the center of the duct cross sectional area. Herein, the COVs are based on the center 12 points covering 75% of the duct cross sectional area. The outer points of the grid are not used because they are too close to the wall, and it is not possible to obtain reliable data with the equipment at hand. Velocity readings at these points with the hot-wire probe register turbulence intensity levels of 40% and higher (Sandborn 1972) owing to the boundary layer and interference from the probe support. This usually leads to tripping of the hot wire anemometer measuring circuits to prevent any damage to them.

The grid for the concentration measurements is based on a refined EPA Method 1 grid that has 32 points. We choose the 20 center points that cover an area slightly less (62.5%) than 2/3 (~67%) of the duct cross sectional area. The difference from the 2/3 (~67%) requirement does not affect the nature of conclusions that are drawn. The outermost sampling location for the 32-point grid is separated from the outermost sampling location for the 16-point grid by a distance of just 2.7 mm in the radial direction. Also, there is an estimated error of 1.5 mm associated with each location on the sampling grid so that within the limits of uncertainty, at the outermost sampling location, the center 2/3 (~67%) of the duct is encompassed. This refined grid is chosen because it has the ability to capture the concentration profiles in more detail than the 16-point grid. Importantly, the relative error at each sampling point is ~11% for the COVs associated with the 32-point grid as compared with a relative error of 24% for the 16-point grid; the relative error for COV being calculated from at least three sets of measurements for a particular inlet condition.

Velocity and tracer gas concentration measurements

The velocity measurements are made with a hot-wire anemometer (Model IFA 100/200, TSI Inc., St. Paul, MN), and the velocity COVs are calculated from the values obtained at the 12 traverse points in the center of the 16-point EPA Method 1 grid. The anemometer samples a total of 2,000 readings within a 2-s period, and parameters like intensity (I) are obtained along with the

time-averaged velocity. The turbulence intensity measurements are also taken at the center of each cross-section area along the duct length for all cases studied. The hot-wire anemometer is calibrated with a pitot tube connected to a micro-manometer (Microtector, Model 1430, Dwyer Instruments Inc., Michigan City, IN) with a least count of 0.0254 mm (0.001 in) gauge of water.

Velocity measurements were made to identify a time T over which readings must be taken in order to compare the experimental data with the numerical results. The time T must be large compared with the integral time scale (time scale over which a variable is correlated with itself; repeated measurements would not yield a stationary time-average). A selection of time $T = 2$ s gives an error for the time averaged velocity that is within 0.3%, and yet allows reliable readings to be obtained in reasonably quick time intervals (Table 1).

Gas concentration tests are conducted by releasing a continuous stream of dilute sulfur hexaflouride (SF_6) gas into the flow. Samples are extracted, over a time period of 2 s, from the locations on the sampling grid (center 20 points of a 32-point EPA Method 1 grid) with 60-mL syringes. The syringes are immediately capped and subsequently analyzed with an electron capture gas chromatograph (Model 101 Autotrac, Lagus Applied Technology Inc., San Diego, CA). The error for the time-averaged concentration is less than 2%. Syringes are flushed prior to every test and a dry sample is taken prior to the actual sample in order to prevent erroneous concentration readings. The reproducibility of results for velocity and tracer gas concentration measurements at a fixed spatial location is also shown by McFarland et al. (1999b).

For tests involving the screen and the bi-plane grids, which resulted in uniform velocity profiles and homogenous inlet turbulence, the gas was released from a single point (center of the duct cross section) immediately downstream of the element involved. For the commercial static gas mixer, three cases were studied. These included release of gas at a single point located at the center either immediately downstream of the mixing device or nearly one diameter before the inlet plane. The other case studied involved gas release at a single point located at a distance, within 20% of the duct diameter, from the wall at the exit plane of the gas mixer. For each case studied, at least three tests are performed and the average COV is calculated.

Table 1. Variation of error in time-averaged velocity with sampling time (T).

Sampling time (T), s	Relative error, %
0.2	0.36
1.0	0.38
2.0	0.28
10.0	0.26

Numerical simulations

In this study, flow field calculations are performed with the Reynold Stress model, however, the k-ϵ model is used whenever stability problems are encountered. Both models are popular for turbulent flow (Rodi 1984). The Lagrangian particle tracking model imbedded in FLUENT is used with the Eulerian flow field that has been calculated using the appropriate turbulence model. We choose, over others, a Stochastic Separated Flow (SSF) model wherein the particle trajectories are generated based on the solution of a particle momentum equation. The dispersive effect of the turbulent fluctuations on the motion of the particles is modeled by a Discrete Random Walk approach. This stochastic method is based on the eddy-lifetime concept and assumes that the velocity fluctuations at any point are maintained over the lifetime of the eddy (Shirolkar et al. 1996).

Mesh generation for the flow field was done using FLUENT, and the mesh contained 15,000 computational nodes. Because of the axisymmetric nature of the flow, only half of the tube needed to be modeled. The velocity profiles at each axial location and the COV profile along the duct length are calculated for the EPA Method 1 grid that is used for the corresponding experimental readings. The tracer gas properties are incorporated by employing small-diameter inertia-less particles. The gas concentration COV was then calculated by tracking the number of particles passing through control volumes located at the center 20 points of the 32-point EPA Method 1 grid.

RESULTS

In this section, the inlet turbulence intensity and the nature of inlet turbulence (homogenous or otherwise) will characterize each test, and, unless mentioned explicitly, the Reynolds number is 15,000. Reynolds number does not have a significant impact on the velocity COV as may be noted from the data given in Table 2. McFarland et al. (1999a) also noted that Reynolds number has little effect and concluded that the mixing is dependent on geometry.

Table 2. Variation of velocity *COV* with Reynolds number (Re) (Inlet intensity = 1.5%).

Downstream location	Re	*COV* (%)
2 D	6,940	2.36
2 D	9,200	2.64
2 D	15,160	2.62

Graphs of velocity COVs at various downstream distances are shown in Figs. 3 and 4 for cases where bi-plane grids were used to setup turbulence intensities of 1.5% and 10% (homogenous) at the inlet of the duct. The experimental results show a trend consistent with the assumption of a (statistically steady) uniform velocity profile evolving towards a fully developed profile. Velocity COV values one diameter downstream of the bi-plane grids are 2.1% and 3.0% for the inlet intensities of 1.5% and 10%, respectively. The velocity COV profile for the case of 20% inlet intensity is not obtained; however, the velocity COV two diameters downstream of the bi-plane grid is 3.2%. Also, for the 20% inlet intensity case, the COV 22 diameters downstream is 11.9%, which is consistent with the results for the inlet intensity of 10%. In all these cases, the final COV varies from 8.2% to 11.9% and is well below the ANSI limit of 20%. This also compares favorably with the value of 7.7% calculated from an established power law profile for fully developed flow at a Reynolds number of 15,000 (Fox and McDonald 1994):

$$\frac{\bar{U}_z}{\bar{U}_{Z(max)}} = \left(1 - \frac{r}{R}\right)^{\frac{1}{5.9}}. \qquad (5)$$

The numerical results of the k-ϵ model and the Reynolds Stress Model for the two cases compare favorably with the experimental data (Figs. 3 and 4). It should be noted that the experimentally-measured inlet COV for velocity for all these cases is not zero, which would be expected for a uniform velocity profile. This is attributed to non-uniformities associated with sampling in the wake of the biplane grids and to errors associated with the measurements.

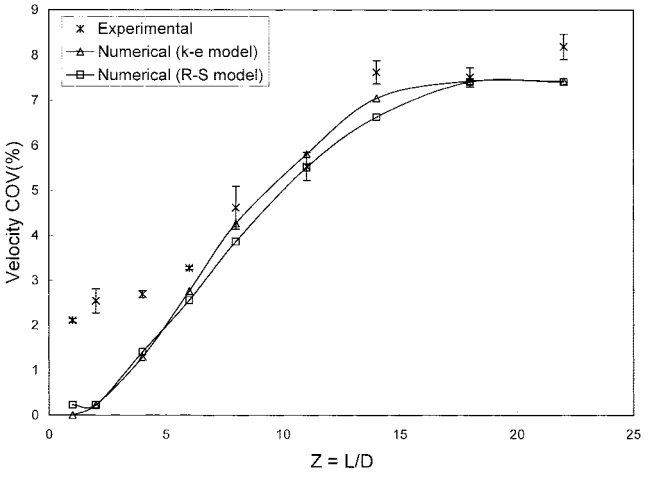

Fig. 3. Velocity COVs at various downstream locations from a bi-plane grid. Inlet turbulence intensity = 1.5%. Error bars represent ±1 standard deviation.

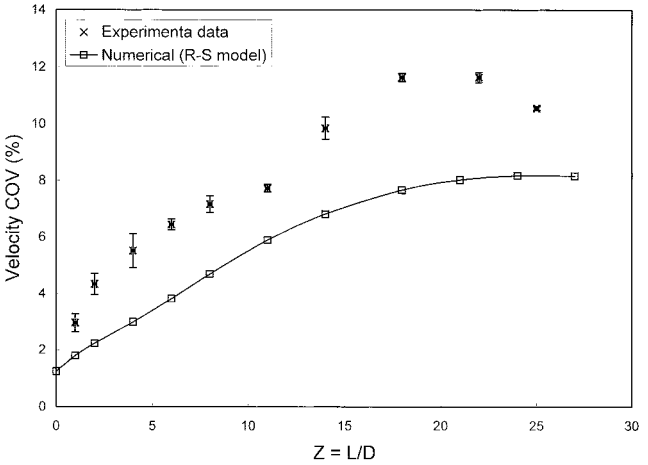

Fig. 4. Velocity COVs at various downstream locations from a bi-plane grid. Inlet turbulence intensity = 10%. Error bars represent ±1 standard deviation.

The tracer gas concentration COV profiles for the cases of 1.5%, 10%, and 20% inlet intensities are shown in Fig. 5. It is intuitive to expect enhanced mixing with increased inlet intensity, and the experimental results bear this out. It is only for an inlet intensity of 20% that the gas concentration COV falls below the ANSI limit of 20% within the duct length studied (27 diameters from the release point). For an inlet intensity of 10%, the gas concentration COV nears the limit of 20% at a distance of 25 diameters from the release point. For an inlet intensity of 1.5% the gas concentration COV is approximately 100% at a distance of 25 diameters from the

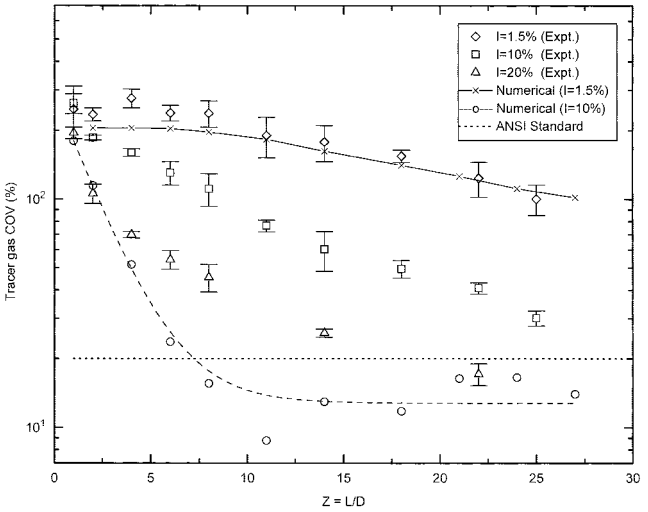

Fig. 5. Tracer gas concentration COVs at various downstream locations from a bi-plane grid. Inlet intensities of 1.5%, 10%, 20%. Error bars represent ±1 standard deviation. Smooth curve fit is drawn for the "Numerical (I=10%)" data.

release location. Theoretically, the COV of gas concentration for molecular species that do not attach to the walls (e.g., SF_6) will approach zero as the distance tends to infinity.

The numerical predictions using the particle-tracking model compare favorably with the experimental data for an inlet intensity of 1.5%. However, the predictions for the case of 10% inlet intensity do not match the experimental data well. The numerical results predict, for example, that the gas COV drops below 20% at about 7 diameters from the release point, whereas the data shows that the COV nears 20% only at 25 to 30 diameters from the release location. The predictions for 20% inlet intensity were not obtained (owing to stability problems with the models) but it is believed that the match between data and predictions would be along lines similar to that for 10% intensity.

In the FLUENT particle-tracking model eddy lifetime (τ_L) can be controlled by a coefficient denoted by c (eqn 6):

$$\tau_L = c\frac{k}{\varepsilon}, \tag{6}$$

where k represents the turbulent kinetic energy, while ε represents the rate of turbulent energy dissipation. The parameter c depends on the turbulence model used and can also be varied based on turbulence intensity. Increasing c leads to increased eddy lifetime and consequently greater mixing. A value of $c = 0.5$ is chosen for the mixing results for an inlet intensity of 1.5%, while a value of $c = 0.3$ is more appropriate for the mixing results for the intensity of 10%. These values are chosen based on the requirements of the code for the turbulence model used for the flow field.

Performance of commercial gas mixer

Enhanced inlet intensity with the bi-plane grids does not meet ANSI mixing requirements in a relatively short distance, so tests were conducted with a commercially available static mixer to determine the degree to which it enhances mixing. The increase in pressure drop due to the inclusion of the mixer is estimated by the manufacturer to be 25 Pa (0.1 inches of water) when the velocity in the duct is 1.4 m s^{-1}. A measurement showed that it was closer to 10 Pa, which is negligible in comparison to a pressure capability on the order of 1,000 Pa for the fans that are used to move air through continuously monitored stacks and ducts. These stacks and ducts are fitted with air pollution control equipment (e.g., HEPA filters), which cause the large pressure drops. Unlike the bi-plane grids, the velocity profile at the exit of the mixer is not uniform, nor is the turbulence homogenous. Hence, apart from the turbulent intensity, the release point of the tracer gas also plays an important role. The results for the three release locations are shown in Fig. 6.

When the tracer gas is released at the center of the exit plane of the gas mixer, the COV falls below the 20% limit at about 22 diameters from the duct inlet. When the release point lies at the center of a plane that is located 1 diameter upstream of the inlet plane of the gas mixer, the COV reaches the 20% value at a distance of 16 to 17 diameters downstream. However, the better results, in terms of the shorter distances to reach ANSI limits, are for the release location at the exit plane of the gas mixer that is at a distance within 20% of the duct diameter from the wall (Fig. 6). The gas concentration COV drops below 20% within 6 to 7 diameters from the exit plane of the gas mixer (also the duct inlet). Another requirement of the ANSI N13.1 1999 Standard, that the maximum value of the concentrations obtained on all points of the EPA grid not be greater than 30% of the average value, is also met.

The radial vanes of the gas mixer ensure introduction of large scale eddies and flow swirl along the outer area of the duct cross-section, and smaller eddies in the central region of the duct cross-section. The high turbulence intensity at the exit plane of the gas mixer decays within 6 diameter lengths. These eddies interact as the flow develops and ensure that the flow is well mixed. Hence, introducing the tracer gas into the larger eddies ensures that the gas is mixed quickly and uniformly. The velocity COV drops from a maximum value at the inlet to a value of 22.8% at the 2-diameter location and to 8.5% at the 22-diameter location.

The velocity profiles at the 22-diameter location correspond to a nearly fully developed flow profile, and there is almost no difference between the velocity profile

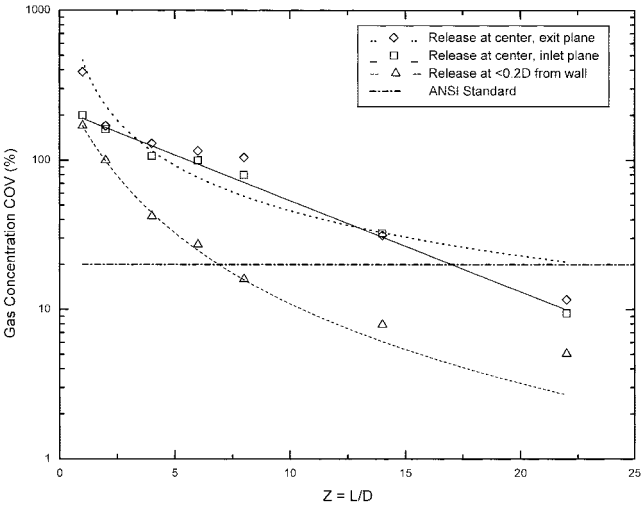

Fig. 6. Tracer gas COV profiles for tests with various release locations for gas mixer.

for an inlet intensity of 10% and the velocity profile with the gas mixer at the inlet. They also compare well with a profile for fully developed flow obtained using an empirical model (eqn 5).

Correlation of gas COV with intensity profile

The principal idea behind the correlation of the gas concentration COV data with the intensity profile is the hypothesis that the intensity, which is related to the turbulent kinetic energy and scale, is the critical factor that determines the extent of mixing, more so than the Reynolds number. A higher intensity (at the inlet) leads to a greater scale of turbulence leading to enhanced mixing. Gupta (1999) and McFarland et al. (1999a, b) found that the variation of mixing, due to Reynolds number, is negligible. In our case, the variation of velocity COV over the low Reynolds number range from 6,000 to 16,000 is verified to be negligible (Table 2). It is concluded that the Reynolds number does not play a very significant role in the gas mixing process, and the effect of turbulent intensity on mixing, at constant Reynolds number, is studied.

The experimental data shows that the gas concentration COV curve drops steeply in the first few diameter lengths from the gas release point and has a gradual gradient beyond this initial distance. This behavior can be tied to the evolution of the (average) turbulence intensity along the duct. The average turbulent intensity is obtained at each cross-sectional location from the values at the 12-point EPA Method 1 grid.

The gas concentration COV is correlated with the averaged turbulent intensity. The model is developed based on the concept of eddy diffusivity, and the assumptions are outlined below. The model has restricted applicability because effects like flow swirl or separation are not captured. It is developed for the case where turbulent intensity is the primary mechanism driving mixing. Starting with the general diffusion equation (eqn 7) and given that there is no generation of the gas constituent, we assume an axi-symmetric variation of concentration (c_{SF6}) with $D_{SF6\text{-air}}$ being the molecular diffusion coefficient:

$$(\rho \vec{U} \cdot \nabla c_{SF6}) - div(D_{SF6\text{-air}} \nabla c_{SF6}) = 0. \qquad (7)$$

Additional approximations, based on experimental data, include neglecting the concentration gradient along the duct length and also the terms due to molecular diffusion.

Each variable in the resulting equation is split into a time-averaged component and a fluctuating component. The equation is then time-averaged to yield

$$\overline{U_z}\frac{\partial \overline{c_{SF6}}}{\partial z} + \overline{U_r}\frac{\partial \overline{c_{SF6}}}{\partial r} + \frac{\partial \overline{u_z' c_{SF6}'}}{\partial z} + \frac{\partial \overline{u_r' c_{SF6}'}}{\partial r} = 0. \qquad (8)$$

A further approximation is that the turbulent transport of the gas (as represented by its concentration) varies steeply in the radial direction as compared to its variation along the duct length. The details of the model are discussed by Mohan (2001). The simplified equations are integrated to yield a model similar to that suggested by Langari (1997). The model (eqn 9) allows us to account for the effect of the history of the intensity variations in predicting the current extent of gas mixing:

$$COV = COV_o \left\{ \exp\left[\frac{-1.5}{D^2} \frac{l_m}{\sigma_t} \int_0^z I(l) dl \right] \right\}^{1/2}. \qquad (9)$$

Here D is the pipe diameter, l is length along the tube, σ_t is the turbulent Prandtl number (a constant for most flows; we use $\sigma_t = 0.7$, the value for a round jet (Rodi 1984)), and l_m is the characteristic (Prandtl) mixing length in the pipe. The parameter l_m is determined empirically for complex flows, but in our simple case we use a constant value for the mixing length calculated to be 0.12 mm (Rodi 1984). This is a simplification because l_m can vary along both the length and diameter of the pipe. However, in our calculation for the gas COV, we use an average value (determined along with the velocity measurements) for the turbulent intensity at each cross-sectional location, $I(l)$, and hence the assumption of a constant mixing length is justified. The predictions of the new model compare favorably with experimental data (Fig. 7). For example, the new model predicts a gas COV of 140% at the 22-diameter location comparable to the experimental average of 125%.

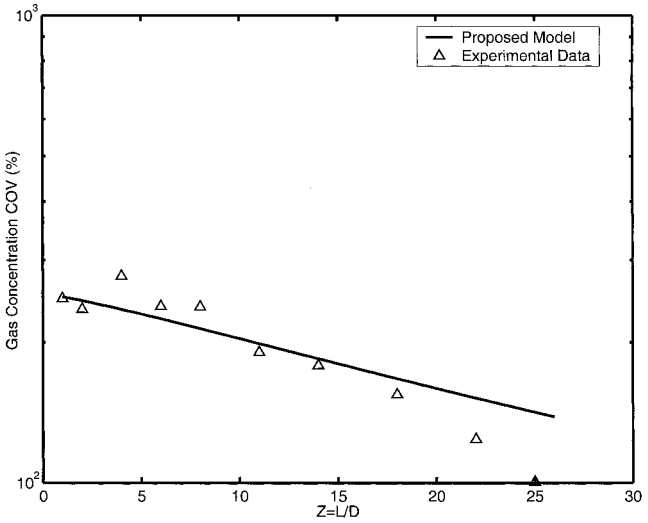

Fig. 7. Comparison of results of proposed model with experimental data for inlet intensity of 1.5%.

Table 3. Reproducibility of COVs from tests with inlet intensity of 20%.

Downstream location	Parameter	Mean COV	Standard deviation of COV values	Relative precision
1D	Gas	263.00%	31.40%	0.119
	Velocity	3.00%	0.42%	0.14
4D	Gas	160.30%	7.54%	0.047
	Velocity	5.52%	0.88%	0.16
11D	Gas	76.60%	6.12%	0.08
	Velocity	7.72%	0.19%	0.025
18D	Gas	49.60%	6.51%	0.131
	Velocity	11.64%	0.20%	0.017
22D	Gas	40.80%	3.48%	0.085
	Velocity	11.64%	0.26%	0.022
			Average of all values:	0.0826

DISCUSSION OF ERRORS

The errors associated with the measurements are recorded, and the reproducibility and reliability of the obtained data is verified. Individual readings of velocity and tracer gas concentration have relative precision levels of ±3.6% and ±3.0%, respectively. The accuracy of the velocity measurements made by the hot-wire anemometer is set by the accuracy of the manometer used to calibrate the sensor. In this case, the accuracy of the velocity readings is about 1 to 2%. The electron gas capture chromatograph is calibrated daily with a calibration gas, and the system is used for the SF_6 concentration range of 0.18 to 50 ppb. The calibration error (relative difference between calibration gas concentration and instrument reading) was within 4% for the range of 0.5 to 21 ppb, and was within 10% for the range of 0.18 to 50 ppb. The manufacturer reported zero calibration error at 5 ppb, and this was the target gas concentration in the experiments. The calibration gas had a relative precision of ±2%, i.e., around 0.1 ppb error for a concentration of 4.92 to 5 ppb. This set the accuracy of the concentration readings to within 0.05 ppb. The background noise of the instrument was around 0.04 ppb in the 0.1 to 10 ppb range, 0.06 ppb in the 10 to 20 ppb range, and around 0.08 to 0.1 ppb for readings greater than 20 ppb.

The velocity and gas concentration COVs (I=20%) at a few locations are documented in Table 3. The relative precision of the tracer gas COV at any location varies between 5% to 16%; a COV value of 10% would thus have a standard deviation of 0.5% to 1.6%. The relative precision of the velocity COV, obtained at any location, varies between 1% to 5%. This is a useful measure to check the reproducibility of the data and trends obtained, especially for this study where the COV value regularly exceeds the 20% standard.

Acknowledgments—This work has been carried out with funding from Westinghouse Savannah River Company (WSRC) to the Texas A&M Research Foundation under subcontract AB62859. Brent Blunt is the WSRC technical representative for the project. The authors wish to thank Luoyi Tao for his efforts related to the numerical results presented herein.

REFERENCES

Abuzeid S, Busnaina AA, Ahmadi G. Wall deposition of aerosol particles in a turbulent channel flow. J Aerosol Sci 22:43–62; 1991.

American National Standards Institute. Guide to sampling airborne radioactive materials in nuclear facilities. New York: ANSI; ANSI Standard N13.1; 1969.

Baker JR. Motionless mixers stir up new uses. Chem. Eng. Progress 87:32–38; 1991.

Cybulski A, Werner K. Static mixers—Criteria for applications and selection. Int Chem Eng 26:171–180; 1986.

Fox RW, McDonald AT. Introduction to fluid mechanics. New York: John Wiley; 1994.

Gupta, R. Turbulent mixing and deposition studies for single point aerosol sampling. College Station, TX: Texas A&M University; 1999. Dissertation.

Hampl V, Niemela R, Shulman S, Bartley DL. Use of tracer gas technique for industrial hood efficiency evaluation—Where to sample? Am Ind Hyg Assoc J 47:281–287; 1986.

Health Physics Society. Sampling and monitoring releases of airborne radioactive substances from the stacks and ducts of nuclear facilities. McLean, VA: HPS; ANSI N13.1; 1999.

Langari A. Turbulent mixing in ducts, theory and experiment application to aerosol single point sampling. College Station, TX: Texas A&M University; 1997. Thesis.

Laws EM, Livesey JL. Flow through screens. Ann Rev Fluid Mech 10:247–266; 1978.

McFarland AR. Methodology for sampling effluent air from stacks and ducts of the nuclear industry. Los Alamos, NM: Los Alamos National Laboratory; Report LA-UR-96–2958; 1998.

McFarland AR, Gong H, Muyshondt A, Wente WB, Anand NK. Aerosol deposition in bends with turbulent flow. Environ Sci Technol 31:3371–3377; 1997.

McFarland AR, Anand NK, Ortiz CA, Gupta R, Chandra S, McManigle AP. A generic mixing system for achieving conditions suitable for single point representative effluent air sampling. Health Phys 76:17–26; 1999a.

McFarland AR, Gupta R, Anand NK. Suitability of air sampling locations downstream of bends and static mixing elements. Health Phys 77:703–712; 1999b.

McFarland AR, Rodgers JC. Single-point representative sampling with shrouded probes. Los Alamos, NM: Los Alamos National Laboratory; Report LA-12612-MS; 1993.

Mohan A. A study on the effect of inlet turbulence on gas mixing for single-point aerosol sampling. College Station, TX: Texas A&M University; 2001. Thesis.

Pahl MH, Muschelknautz E. Static mixers and their applications. Int Chem Eng 22:197–205; 1982.

Rodgers JC, Fairchild CI, Wood GE, Ortiz CA, Muyshondt A, McFarland AR. Single point aerosol sampling: evaluation of mixing and probe performance in a nuclear stack. Health Phys 70:25–35; 1996.

Rodi W. Turbulence models and their application in hydraulics—a state of the art review. Karlsruhe, Federal Republic of Germany: University of Karlsruhe; 1984.

Sandborn VA. Class notes for experimental methods in fluid mechanics. Fort Collins, CO: Colorado State University; 1972.

Shirolkar JS, Coimbra CFM, McQuay MQ. Fundamental aspects of modeling turbulent particle dispersion in dilute flows. Prog Energy Combust Sci 22:363–399; 1996.

U.S. EPA. Letter from Mary D. Nichols, Assistant Administrator for Air and Radiation, U.S. EPA, to Raymond F. Pelletier, Director, Office of Environmental Guidance, U.S. DOE, dated November 21; 1994.

U.S. EPA. Method 1—Sample and velocity traverses for stationary sources, 40CFR60, Appendix A. Washington, DC: U. S. Government Printing Office; 2001a.

U.S. EPA. Method 2—Determination of stack gas velocity and volumetric flow rate (Type S Pitot Tube), 40CFR60, Appendix A. Washington, DC: U. S. Government Printing Office; 2001b.

U.S. EPA. National emission standards for radionuclides other than radon from Department of Energy Facilities, 40CFR61, Subpart H. Washington, DC: U. S. Government Printing Office; 2001c.

U.S. EPA. National emission standards for radionuclide emissions from federal facilities other than nuclear regulatory commission licensees and not covered by Subpart H, 40CFR61, Subpart I. Washington, DC: U. S. Government Printing Office; 2001d. (Available at http://www.access.gpo.gov/nara/cfr/index.html. Accessed 20 March 2002).

APPENDIX

List of Symbols

c_{SF6} = (Instantaneous) tracer gas concentration (mol m^{-3});

c_{SF6}' = Fluctuating component of tracer gas concentration (mol m^{-3});

COV = Coefficient of variation (%);

D = Diameter of pipe (m);

$D_{SF6\text{-}air}$ = Molecular diffusion coefficient (SF_6-air) (m^2 s^{-1});

I = Turbulence intensity (%);

k = Turbulent kinetic energy (m^2 s^{-2});

l = Length along pipe (m);

l_m = Characteristic mixing length (m);

r = Radial coordinate (m);

R = Radius of pipe (m);

U_r = (Instantaneous) velocity along 'r' coordinate (m s^{-1});

$\bar{U}_r$ = (Time-averaged) velocity along 'r' coordinate (m s^{-1});

u'_r = Fluctuating component of velocity along 'r' coordinate (m s^{-1});

U_x = (Instantaneous) velocity along 'x' coordinate (m s^{-1});

$\bar{U}_x$ = (Time-averaged) velocity along 'x' coordinate (m s^{-1});

u_z' = Fluctuating component of velocity along 'z' coordinate (m s^{-1});

z = Axial (along pipe length) coordinate (m).

Greek Letters

ε = Rate of dissipation of turbulent kinetic energy (m^2 s^{-3});

ρ = Density of tracer gas (kg m^{-3});

σ_t = Turbulent Prandtl number (dimensionless);

τ_L = Eddy lifetime (s).

■ ■